

On the Surface Diffusion of Adsorbable Gases Through Porous Media

MARTA PONZI

JOSE PAPA

JUAN B. P. RIVAROLA

and

GIORGIO ZGRABLICH

Universidad Nacional de San Luis
San Luis, Argentina

A model is proposed for the hopping mechanism of surface diffusing molecules, adsorbed on porous solids, which allows a simple calculation of the mean hopping distance as a function of surface coverage.

Surface permeabilities calculated with this model are compared to new experimental data. A satisfactory agreement is obtained, and the values of the parameters involved turn out to be very reasonable.

SCOPE

The most commonly used models to describe the surface diffusion of physically adsorbed gases on porous solids are essentially the following.

1. Fick's law, which considers the surface flux as being proportional to the concentration gradient, the proportionality constant being the diffusion coefficient. Several authors (Higashi et al., 1963; McIntosh, 1966; Perkinson, 1965; Sladek, 1967) introduced a number of corrections to take into account the dependence of the diffusion coefficient on the surface concentration of the adsorbate.

2. Hydrodynamic model, which pictures the adsorbed gas as being a liquid film slipping on the solid surface with a laminar flow (Flood et al., 1952; Gilliland et al., 1958; Babbitt, 1950).

3. Mechanistic model, principally developed by Smith and Metzner (1964) and Weaver and Metzner (1966), which is based on a kinetic study of the hopping movement of adsorbed molecules along the solid surface.

These models show different degrees of validity for different regions of surface coverage values (Horiguchi et al., 1971), and, in general, we believe that a reliable theory for the interpretation and prediction of surface fluxes is still lacking.

The purpose of the present work is to improve the mechanistic model introducing a simple method of calculating the mean hopping distance of an adsorbed molecule, to obtain new experimental data on surface diffusion, and to compare them with the theoretical model.

CONCLUSIONS AND SIGNIFICANCE

The hopping mechanism which we propose to describe surface diffusion permits a simple calculation of the mean hopping distance as a function of surface coverage which satisfactorily fits our experimental results on surface permeability.

The essential parameter of this mechanism is the probability that an activated molecule is captured when it

passes over an empty site. This probability evidently depends on the adsorption potential at each site, and we believe that this is a starting point toward a correct treatment of diffusion on energetically heterogeneous surfaces.

A microphysical model to predict the dependence of activation energy on surface coverage is still lacking. However, an empirical relation is also proposed which seems to fit satisfactorily our experimental data.

BASIC KINETIC EQUATIONS

According to Smith and Metzner (1964) and Weaver and Metzner (1966), the calculation of the surface flux is based on the following hypothesis.

1. The gaseous and adsorbed phases, both composed of a single gas, are in thermodynamical equilibrium characterized by adsorption isotherms.

2. Adsorbed molecules migrate along the adsorbent sur-

2. As the rate of partial desorption decreases exponentially with the activation energy, Equation (2), a molecule adsorbed in a potential well will preferably migrate through one of the four neighboring valleys to a new potential well.

3. If the new potential well is already occupied by another molecule, the activated molecule will continue its random migration through one of the four neighboring valleys.

4. If the new potential well is empty, then the activated molecule will have a probability g of being captured and a probability $1 - g$ of continuing its migration.

5. The process goes on until the activated molecule is readsorbed at some potential well after describing, for example, a trajectory like the one shown in Figure 1.

Under these assumptions it is possible to obtain values of λ^2 as a function of θ for different values of g by means of Monte Carlo simulation.

For the numerical simulation we used a square array with 2500 sites, and the results are shown in Figure 2. We can see immediately that the growth of λ^2 as θ increases is quite pronounced and is greater as g decreases.

If we neglect recurrence to the origin effects and assume that each hop is completely independent from the previous one, then it is possible to obtain an approximate analytical expression for the function $\lambda^2(\theta)$. In fact, under these simplifications the problem reduces to one of a bidimensional random walk with an effective probability

$$P_{ef} = g(1 - \theta) \quad (7)$$

that a molecule be captured when passing over a potential well and a probability $1 - P_{ef}$ of continuing its migration.

Then, if \vec{r}_i is the translation unitary vector corresponding to the i^{th} step, we have

$$\lambda^2 = \left\langle \left[\sum_{i=1}^n \vec{r}_i \right]^2 \right\rangle = \left\langle \sum_{i \neq j} \vec{r}_i \cdot \vec{r}_j \right\rangle + \left\langle \sum_{i=1}^n |\vec{r}_i|^2 \right\rangle = \left\langle \sum_{i=1}^n |\vec{r}_i|^2 \right\rangle = \bar{n} \quad (8)$$

where $\langle F \rangle$ stands for the mean value of any function F and \bar{n} is the mean number of steps that a molecule undergoes from its activation until its readsorption.

To obtain \bar{n} we need the probability P_n that a molecule undergoes exactly n steps in its activated state. This is given by

$$P_n = (1 - P_{ef})^{n-1} P_{ef} \quad (9)$$

Then

$$\bar{n} = \sum_{n=0}^{\infty} n P_n = P_{ef} \sum_{n=0}^{\infty} n (1 - P_{ef})^{n-1} = \frac{1}{P_{ef}} \quad (10)$$

Finally, from Equations (7), (8), and (10), and for a array of spacing d , we have

$$\lambda^2 = \frac{d^2}{g(1 - \theta)} \quad (11)$$

The comparison of this approximation with the Monte Carlo results is also shown in Figure 2. As we can see, the approximation given by Equation (11) is quite satisfactory up to considerably high values of θ . At least we can use it up to $\theta = 0.65$.

EXPERIMENTAL RESULTS

The experimental apparatus used to obtain permeability values is outlined in Figure 3. The pressure in the high

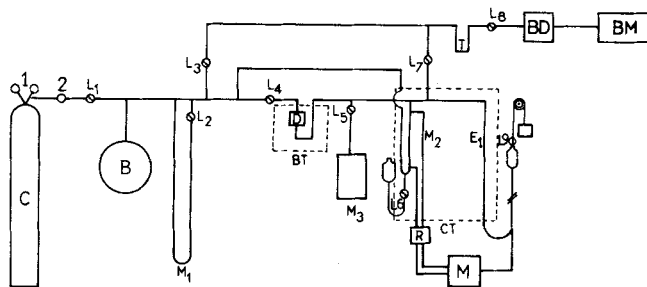


Fig. 3. Experimental apparatus.

pressure region (to the left of the diffusion cell D) is kept constant owing to its high volume, while the pressure in the low pressure region (to the right of D) is kept constant by increasing its volume by means of the displacement of a mercury column (Ross and Good, 1956; Villet and Wilhelm, 1961). In this way the volume increase necessary to keep the pressure constant as a function of time is obtained, and then the volumetric flux and the permeability are obtained.

The apparatus includes a cylinder C which contains the gas to be used, a bulb B (1 000 cm³) to increase the volume in the region, a diffusion cell D which contains the porous solid pellet, the pressure gauges M₁ to measure the internal pressure, M₂ to measure the pressure difference between the two sides of the pellet, and the McLeod gauge M₃ to measure the degree of vacuum reached. Also included are a volume measuring burette E₁, a cold trap T, a vacuum system with mechanical and diffusion pumps BM and BD, a thermostatic bath BT to keep the diffusion cell

TABLE 1. PROPERTIES OF CARBON REGAL 660

- A. Powder
 - Density = 1.8 g/cm³
 - Monolayer volume for Freon 12, $V_m = 24.5$ cm³/g
 - Specific surface, $S_w = 106 \times 10^4$ cm²/g
- B. Pellet
 - Diameter = 0.99 cm
 - Length = 0.6 cm
 - Transverse area = 0.77 cm²
 - Density, $\rho_p = 1.061$ g/cm³
 - Porosity, $\epsilon = 0.41$
 - Mean pore radius, $\bar{r} = 87.5$ Å
 - Tortuosity factor, $\tau_g = 1.22$

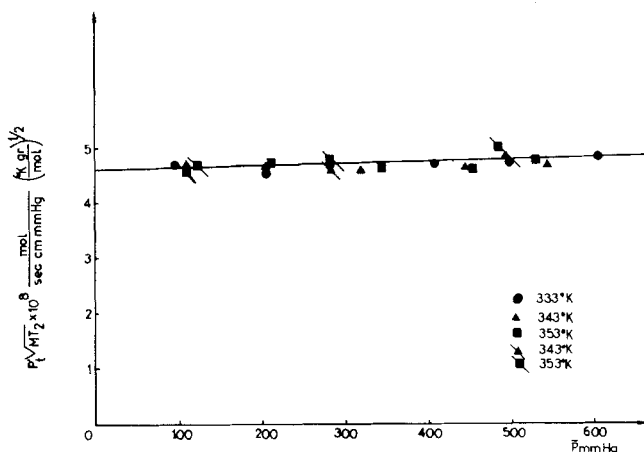


Fig. 4. Total permeability for Nitrogen as a function of pressure at several temperatures.

at constant temperature, and a thermostatic chamber CT to keep the burette E₁ at constant temperature. Finally, a relay R and a motor M keep constant the pressure in the low pressure region by lowering the mercury level in the burette E₁ when a platinum contact in the differential manometer M₂ is disconnected as the pressure increases owing to the diffusion of gas through the pellet. The volumetric flux is then electronically recorded.

The adsorption isotherms were measured on a classical gravimetric apparatus.

The porous solid used was Carbon Regal 660, provided by Cabot, and the measurements of its physical characteristics such as apparent density ρ_p , specific surface S_w ,

porosity ϵ , and mean pore radius \bar{r} yielded the values shown in Table 1.

To determine the contribution of the nonadsorbed phase to the total permeability, volumetric fluxes were measured using as diffusing gas pure (99.99%) nitrogen at temperatures of 333°, 343°, and 353° K. The results are shown in Figure 4.

We see that $P'_t\sqrt{MT}$, where P'_t is the total permeability and is constant at the three temperatures and over a large pressure range, which means that there is no surface transport and that the diffusion in this case was of the Knudsen type, and the value of $P'_G\sqrt{MT}$, where P'_G is the permeability due to the gaseous or nonadsorbed phase, was (4.6

TABLE 2. SURFACE PERMEABILITIES FOR FREON 12

T, °K	p, mmHg	θ	$P'_t\sqrt{MT_2}$	$(P'_G)_c\sqrt{MT_2}$	$P'_s\sqrt{MT_2}$	P'_s
			(g-mole °K g) ^{1/2} /cm s mmHg			g-mole
			10 ⁸	10 ⁸	10 ⁸	cm s mmHg 10 ¹⁰
268	12.9	0.139	9.67 ± 0.38	4.45	5.22	2.90 ± 0.48
268	21.8	0.192	9.17 ± 0.34	4.39	4.78	2.66 ± 0.44
268	30.6	0.227	9.32 ± 0.36	4.35	4.97	2.76 ± 0.47
268	31.2	0.227	8.72 ± 0.24	4.35	4.37	2.43 ± 0.35
268	47.7	0.282	8.53 ± 0.30	4.29	4.24	2.36 ± 0.41
268	60.6	0.316	8.14 ± 0.31	4.25	3.89	2.16 ± 0.42
268	85.1	0.359	8.18 ± 0.28	4.20	3.98	2.12 ± 0.39
268	87.2	0.361	8.07 ± 0.28	4.20	3.87	2.15 ± 0.39
268	114.2	0.396	7.57 ± 0.28	4.16	3.41	1.89 ± 0.38
268	191.5	0.461	7.55 ± 0.34	4.09	3.46	1.92 ± 0.45
268	257.8	0.498	7.20 ± 0.33	4.05	3.15	1.75 ± 0.43
268	346.0	0.537	6.90 ± 0.59	4.01	2.89	1.61 ± 0.70
268	376.9	0.549	7.01 ± 0.29	3.99	3.02	1.68 ± 0.40
268	463.0	0.586	6.60 ± 0.62	3.95	2.65	1.47 ± 0.73
283	8.1	0.055	8.48 ± 0.40	4.54	3.94	2.13 ± 0.50
283	15.3	0.092	8.85 ± 0.39	4.49	4.36	2.35 ± 0.50
283	19.4	0.109	8.54 ± 0.30	4.47	4.07	2.20 ± 0.41
283	31.9	0.155	8.18 ± 0.31	4.42	3.76	2.03 ± 0.42
283	41.9	0.184	7.82 ± 0.32	4.39	3.43	1.85 ± 0.43
283	43.5	0.188	7.77 ± 0.30	4.38	3.39	1.83 ± 0.40
283	65.0	0.235	7.40 ± 0.32	4.33	3.07	1.66 ± 0.43
283	73.9	0.251	7.45 ± 0.26	4.31	3.14	1.69 ± 0.36
283	77.3	0.255	7.54 ± 0.28	4.31	3.23	1.75 ± 0.38
283	102.7	0.293	7.27 ± 0.25	4.26	3.01	1.63 ± 0.36
283	109.9	0.302	7.24 ± 0.31	4.25	2.99	1.62 ± 0.41
283	144.7	0.339	7.09 ± 0.30	4.21	2.88	1.56 ± 0.40
283	212.0	0.387	6.93 ± 0.42	4.15	2.78	1.50 ± 0.53
283	250.1	0.406	6.94 ± 0.35	4.13	2.81	1.51 ± 0.45
283	307.0	0.431	6.86 ± 0.33	4.10	2.76	1.49 ± 0.44
283	361.1	0.453	6.58 ± 0.34	4.08	2.50	1.35 ± 0.45
283	388.4	0.461	6.87 ± 0.33	4.07	2.80	1.51 ± 0.44
283	462.7	0.488	6.13 ± 0.43	4.04	2.09	1.13 ± 0.54
313	13.7	0.033	7.28 ± 0.34	4.56	2.72	1.40 ± 0.44
313	18.9	0.043	7.41 ± 0.32	4.55	2.86	1.47 ± 0.43
313	23.1	0.051	7.28 ± 0.32	4.54	2.74	1.41 ± 0.43
313	24.3	0.053	6.82 ± 0.27	4.53	2.29	1.17 ± 0.38
313	25.9	0.057	6.91 ± 0.20	4.53	2.38	1.22 ± 0.31
313	30.6	0.067	7.13 ± 0.28	4.52	2.61	1.34 ± 0.38
313	33.5	0.071	7.07 ± 0.29	4.51	2.56	1.31 ± 0.40
313	40.6	0.084	7.17 ± 0.34	4.50	2.67	1.37 ± 0.45
313	50.4	0.098	6.85 ± 0.26	4.48	2.37	1.22 ± 0.36
313	63.2	0.116	6.91 ± 0.24	4.46	2.45	1.26 ± 0.35
313	65.0	0.120	6.68 ± 0.22	4.46	2.22	1.14 ± 0.33
313	90.5	0.149	6.80 ± 0.25	4.42	2.38	1.22 ± 0.35
313	120.9	0.178	6.58 ± 0.27	4.39	2.19	1.12 ± 0.37
313	193.3	0.235	6.55 ± 0.39	4.32	2.23	1.14 ± 0.50
313	258.4	0.278	6.79 ± 0.36	4.27	2.52	1.29 ± 0.46
313	292.9	0.295	6.67 ± 0.37	4.25	2.42	1.24 ± 0.48
313	411.2	0.336	6.31 ± 0.28	4.20	2.11	1.08 ± 0.39
313	529.8	0.367	6.89 ± 0.39	4.16	2.73	1.40 ± 0.50

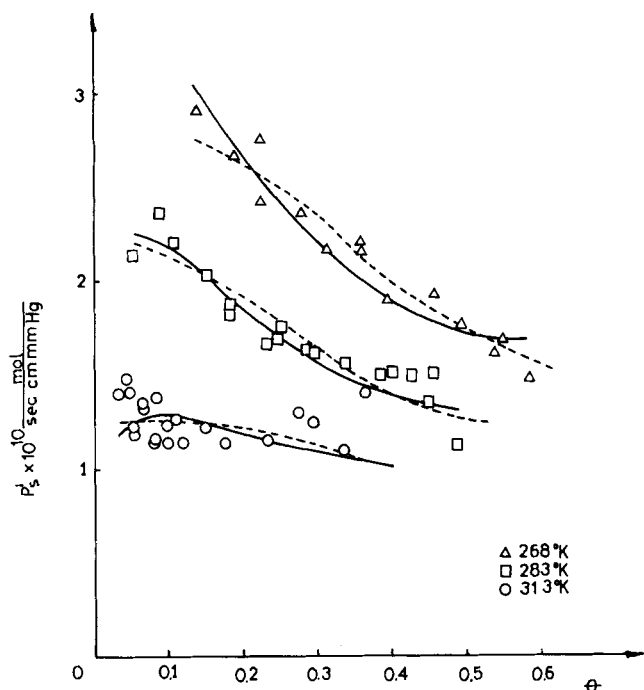


Fig. 5. Surface permeability for Freon 12. Lines correspond to the fits obtained by using Equation (13). Dashed lines correspond to Equation (16).

$\pm 0.1) \times 10^{-8}$ (g-mole/s cm mmHg) (g °K/g-mole) $^{1/2}$.
From this value and the relation

$$P'_G \sqrt{MT} = \frac{2}{3} \sqrt{\frac{8}{\pi R}} \bar{r} \frac{\epsilon}{\tau_g}$$

we get the value of $\tau_g = 1.22$.

Once the contribution of the nonadsorbed phase was established, measurements of adsorption isotherms and total permeabilities for the gas Freon 12 at temperatures of 268°, 283°, and 313°K were carried out. Surface permeabilities P'_s were obtained by subtracting from the total permeabilities P'_t the permeabilities due to the nonadsorbed phase P'_G which were corrected to take into account the decrease of the pore radius \bar{r} due to adsorption. The results are shown in Table 2 and Figure 5.

Adsorption isotherms shown in Figure 6 were fitted by a mean-square procedure with the equation

$$p = k_1 \theta \exp(k_2 \theta + k_3 \theta^2) \quad (12)$$

where k_1 , k_2 , and k_3 are fitting parameters, and then Equation (12) was used to compute $d\theta/dp$ in Equation (5).

ANALYSIS OF RESULTS

In order to improve our knowledge of surface diffusion we must analyze the experimental results in the light of the theoretical model.

For that purpose we use the relation given by Equation (11) in Equation (5).

If we assume, following Smith and Metzner (1964), that ΔF^* is directly proportional to ΔF , the free energy of desorption, and denoting ΔF by the usual logarithmic relationship, we can write

$$\exp\left(-\frac{E^*}{RT}\right) = \frac{Q}{Q^*} \left(\frac{p}{p_o}\right)^a \quad (13)$$

where a denotes the proportionality constant and p_o is a reference pressure.

Substituting Equation (11) and (13) in Equation (5), we obtain

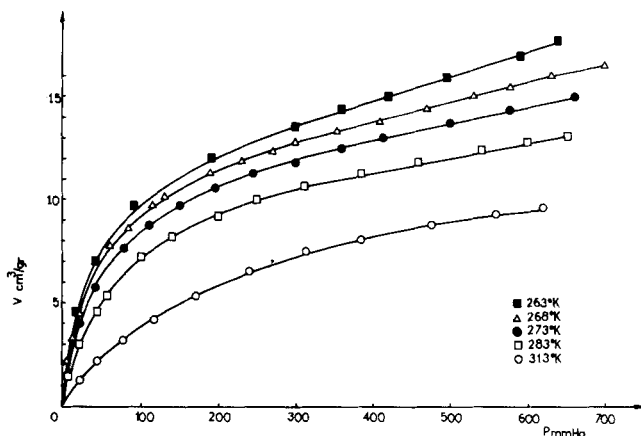


Fig. 6. Adsorption isotherms for Freon 12. Lines correspond to Equation (12).

TABLE 3. FITTING PARAMETERS FOR EQUATION (14)

$T, ^\circ\text{K}$	$\mathcal{M}, \text{g-mole/cm s}$	a	$\frac{1}{g}$
268	488×10^{-7}	0.275	44
283	594×10^{-7}	0.313	50
313	759×10^{-7}	0.286	58

TABLE 4. FITTING PARAMETERS FOR EQUATIONS (5) WITH (11) AND (16)

$T, ^\circ\text{K}$	$\mathcal{M}', \text{g-mole/cm s}$	$a', \text{K-cal/g-mole}$	b'	$\frac{Q^*}{g Q}$
268	808×10^{-7}	2.474	2.280	72
283	1365×10^{-7}	2.509	1.935	116
313	1887×10^{-7}	1.980	1.856	144

$$P'_s = \mathcal{M} \left(\frac{p}{p_o}\right)^a \left\{ \frac{\theta}{(1-\theta)^2} \frac{d\theta}{dp} + \frac{\pi}{2} \frac{1}{(1-\theta)} \left[\frac{d\theta}{dp} + a \frac{\theta}{p} \right] \right\} \quad (14)$$

where

$$\mathcal{M} = \frac{d^2 p_p k T C_{sm}}{2\pi r_g^2 h g} \quad (15)$$

Equation (14) was fitted by the chi-square method to our experimental data. The best values of \mathcal{M} and a are

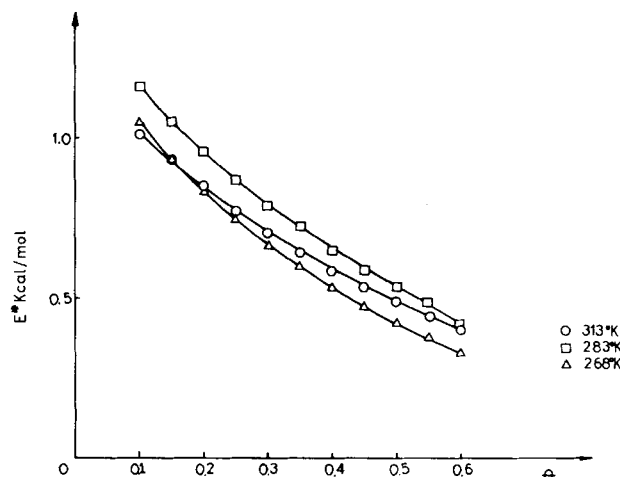


Fig. 7. Activation energy as a function of θ obtained by means of Equation (16).

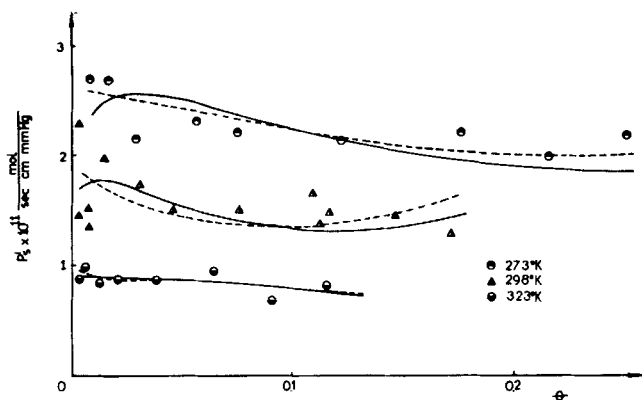


Fig. 8. Surface permeability for Ethane on Vycor, from Horiguchi et al. (1971). Solid line follows the results obtained by using Equation (13) and dashed line by using Equation (16).

shown in Table 3 and the comparison with experimental data in Figure 5. From the values of a , which are about 0.3, we see that the free energy of activation is considerably lower than the free energy of desorption. This result is quite satisfactory, in opposition to the value $a = 1$ obtained by Smith and Metzner (1964).

If, on the other hand, we do not use Equation (13), then we must assume some relation between E^* and θ in Equation (5). We suggest the form

$$E^* = a' e^{-b'\theta} \quad (16)$$

where a' and b' are fitting parameters.

Using this relation, we fitted, by a chi-square method, Equation (5) to our experimental data, obtaining the results of Table 4, where $\bar{M}' = \bar{M}Q^*/Q$, and Figure 5. We see that the new fit is quite similar to the previous one. However, we have now an approximate idea about the dependence of the activation energy E^* on the coverage θ , which is represented in Figure 7. The pronounced decrease of E^* as θ increases is consistent with the fact that the carbon we used is energetically heterogeneous.

Finally, it is possible to estimate the values of the parameters $1/g$ and Q^*/Qg from the values of \bar{M} and \bar{M}' , respectively, obtained in the fits and the value of d^2 which can be calculated from the BET values of S_w and V_m as being 16 \AA^2 . The values of $1/g$ and Q^*/Qg are shown in Tables 3 and 4 for the corresponding values of \bar{M} and \bar{M}' .

We can see, then, that all of the parameters involved have very reasonable values, which makes the model quite satisfactory.

Horiguchi et al. (1971) experimental data of surface permeability for ethane on vycor are shown in Figure 8.

ACKNOWLEDGMENT

This work was supported in part by a grant from the Consejo Nacional de Investigaciones Científicas y Técnicas of Argentina.

NOTATION

- a = constant defined in Equation (13)
- a', b' = constant in Equation (16)
- c = proportionality constant
- C_s, C_{sm} = surface and monolayer surface concentrations, g-mole/g
- d = solid structure constant
- E^* = activation energy, cal/g-mole
- $\Delta F, \Delta F^*$ = desorption and activation free energies, cal/g-mole
- g = adsorption probability
- h = Planck's constant
- k = Boltzmann's constant

- k_1, k_2, k_3 = constant in Equation (12)
- \bar{M} = constant defined in Equation (15), g-mole/cm s
- \bar{M}' = $\bar{M}Q^*/Q$, g-mole/cm s
- M = molecular weight
- M' = defined in Equation (6), $1/^\circ\text{K s}$
- \bar{n} = mean number of steps
- N_A = molar flux of gas A, g-mole/cm² s
- p = pressure, mm Hg
- P_{ef} = effective adsorption probability
- P_n = probability for a molecule to undergo n steps in its activated state
- p_o = reference pressure, equal to 760 mm Hg
- P_G' = gaseous permeability, g-mole/cm s mm Hg
- P_s' = surface permeability, g-mole/cm s mm Hg
- P_t' = total permeability, g-mole/cm s mm Hg
- Q, Q^* = partition functions of adsorbed and activated molecules
- r = rate of partial desorption, g-mole/cm² s
- R = gas constant
- \bar{r} = mean pore radius
- \rightarrow
- r_i = translation vector of the i^{th} step
- S_w = specific surface of the solid, cm²/g
- T = absolute temperature, $^\circ\text{K}$
- V_m = adsorbed volume at monolayer, cm³/g
- z = direction of the net flux

Greek Letters

- ϵ = porosity
- θ = surface coverage
- λ = mean hopping distance
- ρ_p = pellet density, g/cm³
- τ_g = tortuosity factor

LITERATURE CITED

- Babbitt, J. D., "On the Differential Equations of Diffusions," *Can. J. Res.*, **28A**, 449 (1950).
- Flood, E. A., R. H. Tomlinson, and A. E. Leger, "The Flow of Fluids Through Activated Carbon Rods," *Can. J. Chem.*, **30**, 389 (1952).
- Gilliland, E. R., B. F. Baddour, and J. L. Russell, "Rates of Flow Through Microporous Solids," *AIChE J.*, **4**, 90 (1958).
- Glasstone, S., K. J. Laidler, and H. Eyring, *The Theory of Rate Processes*, McGraw-Hill, New York (1941).
- Higashi, K., H. Ito, and J. Oishi, "Surface Diffusion Phenomena in Gaseous Diffusion," *J. Japan Atom. Energy Soc.*, **5**, 846 (1963).
- Horiguchi, Y., R. R. Hudgins, and P. L. Silveston, "Effect of Surface Heterogeneity on Surface Diffusion in Microporous Solids," *Can. J. Chem. Eng.*, **49**, 76 (1971).
- McIntosh, J. R., "Surface Diffusion in Microporous Media at High Surface Coverage," Ph.D. thesis, Dept. of Chem. Eng., Univ. of Iowa, Ames (1966).
- Perkinson, G. P., "Flow of Adsorbed Gases Through Microporous Media," Sc.D. thesis, Dept. of Chem. Eng., Mass. Inst. Technol., Cambridge (1965).
- Ross, J. W., and R. J. Good, "Adsorption and Surface Diffusion of n-Butane on Spheron 6 (2700°) Carbon Black," *J. Phys. Chem.*, **60**, 1167 (1956).
- Roybal, L. A., and S. I. Sandler, "Surface Diffusion of Adsorbable Gases Through Porous Media," *AIChE J.*, **18**, 39 (1972).
- Sladek, K. J., "The Surface Mobility of Hydrogen Chemisorbed on Platinum," Sc.D. thesis, Dept. of Chem. Eng., Mass. Inst. Technol., Cambridge (1967).
- Smith, R. K., and A. B. Metzner, "Rates of Surface Migration of Physically Adsorbed Gases," *J. Phys. Chem.*, **68**, 2741 (1964).
- Villet, J. A., and R. H. Wilhelm, "Knudsen Flow-Diffusion in Porous Pellets," *Ind. Eng. Chem.*, **53**, 837 (1961).
- Weaver, J. A., and A. B. Metzner, "The Surface Transport of Adsorbed Molecules," *AIChE J.*, **12**, 655 (1966).

Manuscript received May 27, 1976; revision received February 11, and accepted February 21, 1977.